

Regulation of Wind Turbine and Battery Direct Current Voltage for Microgrid

Sidiq Budi Perkasa¹, Mochammad Facta¹, Iwan Setiawan¹

¹ Department of Electrical Engineering, Faculty of Engineering, Universitas Diponegoro, Semarang, Jawa Tengah 50275, Indonesia

[Submitted: 9 July 2024, Revised: 23 September 2024, Accepted: 4 November 2024]
Corresponding Author: Sidiq Budi Perkasa (email: sidiqbudi22@gmail.com)

ABSTRACT — Renewable energy will eventually replace fossil energy. Direct current (dc) microgrids can operate independently without being connected to the utility grid. The configuration of a dc microgrid system may encompass wind turbines, permanent magnet synchronous generators (PMSG), rectifiers, dc-dc boost converters, bidirectional dc-dc converters, batteries, and maximum power point tracking (MPPT). Systems with complex components have the problem of maintaining a stable dc voltage amid a load or wind speed change. This paper focuses on improving the performance of dc microgrids by adding voltage control to satisfy the load demand and maintain a constant dc voltage stability. Tests were conducted under three conditions. In the first condition, the wind turbine may supply the load and battery; in the second condition, the wind turbine and battery supply the load; and in the third condition, the battery fully supplies the load. The test results showed that the performance of the designed system could satisfy the load demand and charge the battery. When the wind turbine generators were unable to satisfy the load demand, the battery and wind turbine could supply the load. The system could maintain a voltage on the dc bus of 400 V, with a deviation of only 1%. According to the IEC 61000-14-17, this value remains within the acceptable load tolerance limit.

KEYWORDS — Battery, MPPT, PI Controller, Converter, Wind Turbine, Direct Current Microgrid.

I. INTRODUCTION

The demand for electricity escalates as Indonesia's population increases. One of the largest renewable energy resources is wind energy. The Ministry of Energy and Mineral Resources (Energi dan Sumber Daya Mineral Republik Indonesia, ESDM) asserts that Indonesia has a wind energy potential of 60.65 GW because Indonesia is an archipelagic country with numerous coastal areas possessing sufficient potential for power generation. The direct current (dc) microgrid is an excellent way to harness renewable energy sources and is a viable solution to address the growing demand for electricity loads [1]. There are several types of microgrids, including alternating current (ac) microgrids, dc microgrids, and combined microgrids (ac/dc). The dc microgrids are superior to ac microgrids due to numerous advantages, resulting in significant attention for their development [2], [3].

The advantages of dc microgrid are its reliable system, simpler structure, better performance, and higher converter efficiency [4], [5]. In the future, renewable energy will be the source of electricity, replacing fossil energy. Microgrids can operate independently without being connected to the utility grid. This technique is commonly used in areas that are outside the utility grid. However, an ideal control strategy for dc-dc converters is required to improve the performance of the dc microgrid. This control is needed because many converters in the dc microgrid are connected in parallel to supply the load [6].

One of the most promising renewable energy sources is wind energy. The kinetic energy of the wind is converted into electrical energy using wind turbines through a rotating rotor connected to a generator. These wind turbines can be installed in various locations, from onshore to offshore waters, depending on their design and capacity. Nevertheless, the dynamic characteristics of the wind result in the slower reaction of the power that can be absorbed by wind power plants. As a result, it is hard to maintain maximum power [7]. Various efforts can be made to optimize wind turbines, ranging from

blades, generators, to controllers. Wind turbines require technology that can enhance their system reliability in altering wind conditions. One such technologies is the maximum power point tracking (MPPT) controller. MPPT tracks the power generated by wind turbines to achieve their maximum point under variable wind conditions [8]. One of the most widely used methods of MPPT is perturb & observe (P&O). This algorithm manipulates the duty cycle value of the converter to continuously increase or decrease the voltage of the wind turbine based on the previous power value until it reaches the maximum power point.

The dc-dc converter regulates the energy flow from the renewable energy source to the load and energy storage on the dc microgrid. In a dc microgrid utilizing wind turbines without energy storage, the energy supply to the load will be cut off despite the utilization of the MPPT to generate maximum output power. As a result, microgrid systems require technology that can enhance system reliability. The solution is to provide electrical energy storage technology from backup energy sources [9], [10]. To enhance the reliability of the microgrid system, a bidirectional dc-dc converter with a battery as an energy storage component can be employed to store the energy produced by wind turbines. Bidirectional dc-dc converters have two operating modes: battery charging mode and battery discharge mode [11]. A battery will store excess energy when its capacity produces more energy than the load demands. Conversely, when its capacity produces less energy than the load demands, the energy stored in the battery will be used. Thus, this paper addresses the difficulties of maintaining a stable power supply to the load when there is a change in load or in wind speed.

There have been several previous studies regarding dc microgrid configuration and converter design. In some scientific works, researchers have investigated various renewable energy sources, including hydro, solar, wind, tides,

biomass, biogas, and geothermal [12]–[14]. Due to the stochastic nature of renewable energy sources, the utilization of such energy sources requires a combination of storage devices. In general, previous research findings suggest that algorithmically optimized bidirectional dc-dc converters can improve efficiency [15], [16]. Based on previous research, the passive control method on a bidirectional dc-dc converter connected to a battery for voltage regulation in a dc microgrid cannot dynamically respond to load changes [17]. This research designed a voltage regulation system for wind-battery turbine-based dc microgrids with a bidirectional topology employing PI-based voltage control to ensure voltage stability and fulfill load demands.

II. SYSTEM CONFIGURATION

Figure 1 presents the block diagram of the design of the wind turbine-battery-based dc microgrid voltage regulation system. This system comprises the wind turbines, permanent magnet synchronous generators (PMSG), rectifiers, dc-dc boost converters, bidirectional dc-dc converters, MPPT, proportional-integral (PI) control, battery, and dc load.

A. WIND TURBINES

The uneven heating of the earth by the sun has made wind energy an alternative that can be utilized by humans to generate electricity [18]. Wind turbines, also dubbed windmills, are tools that can convert alternative energy, namely wind, to electrical energy. The working principle of the wind turbines is that the wind speed generates mechanical energy (rotation), which is subsequently being utilized as the generator drivers. The amount of wind power harvested by the turbine depends on the size of the turbine blades and the wind speed in an area [18]. Equation (1) can be used to calculate the wind power (P_w).

$$P_w = \frac{1}{2} \pi R^2 \rho v^3 \quad (1)$$

with R being the spokes of a wind turbine, ρ being the air density, and v being the wind speed. Equation (2) can be employed to formulate the generated mechanical power (P_m).

$$P_m = \frac{1}{2} C_p \pi R^2 \rho v^3 \quad (2)$$

where C_p is the power coefficient (%) [18].

According to the Betz limit, the maximum efficiency of a wind turbine is 0.57. The power coefficient (C_p) and tip speed ratio (TSR) (λ) determine the mechanical power. TSR is the ratio of turbine and wind speed, while power coefficient is the ratio of mechanical and wind power [18]. Equation (3) is used to calculate the power coefficient (C_p), whereas TSR (λ) can be calculated using (4).

$$C_p = \frac{P_m}{P_w} \quad (3)$$

$$\lambda = \frac{\omega_w R}{v} \quad (4)$$

Parameters used in this research are shown in Table I. The mechanical output power is 3,000 W, the base wind speed is 12 m/s, the maximum power at the base wind speed is 1 p.u., while the basic rotation speed of the generator is 1.3 p.u. The pitch angle used is 0°.

B. PERMANENT MAGNET SYNCHRONOUS GENERATOR (PMSG)

Generators are tool that can convert mechanical to electrical energies. If the voltage (V) equals to current (I), generators

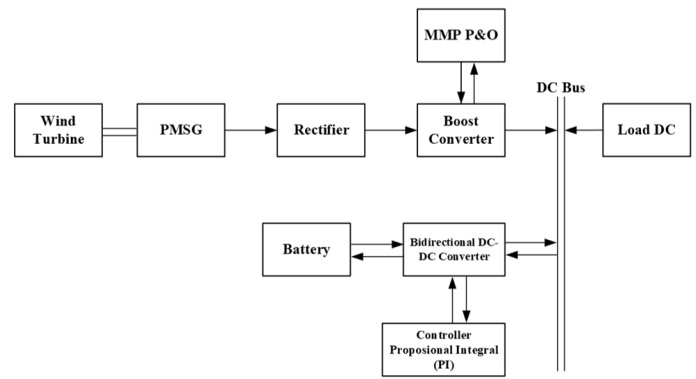


Figure 1. Block diagram of the system.

convert torque (T) and rotor rotation speed (ω). When employed in the wind turbines with low to medium power capacity, PMSG usually produces 3-phase ac electricity. In this research, preset model number 6 was used on the Simulink MATLAB. PMSG generator parameters used is presented in Table II.

C. RECTIFIER

Wave rectifiers are composed of diode that function as the ac to dc wave. The diode allows half of the wave to pass through when the ac flows, while blocking the other half of the wave [19]. In this system design, a half-wave rectifier was used with a single diode to stop the negative signal side of the PMSG ac output wave and skip the positive signal side. Furthermore, the rectifier parameters used were a snubber resistance of 100,000 Ω , a forward voltage of 0.8 V, a power electronic device used a diode, and three bridge arms.

D. BOOST CONVERTER

One type of dc converter is a dc-dc boost topology converter that increases the input voltage to a higher output voltage. A boost converter consists of an inductor (L), an active switch component such as a MOSFET or insulated-gate bipolar transistor (IGBT) (Q), a diode as a passive switch (D), and a capacitor (C). The inductor in the boost converter circuit is used to store energy in the form of current, while the capacitor is used as a filter to reduce the output voltage ripples [20]. Figure 2 shows a model of the boost converter network. The parameters of the boost converter used were a switching frequency (f_s) of 5,000 Hz, an inductor (L) of 0.0750 H, and a capacitor (C) of 0.46875 F.

In buck mode, the relationship between the output voltage (V_o) and the input voltage (V_s) are shown in (5).

$$V_o = 1 - \frac{V_s}{D} \quad (5)$$

The output capacitor (C) and minimum inductor (L_{min}) values of buck converters are expressed by (6) and (7).

$$L_{min} = \frac{(1-D)^2 * D * R}{2 * f} \quad (6)$$

$$C_{min} = \frac{D * V_{out}}{V_r * R * f} \quad (7)$$

E. PERTURB AND OBSERVE (P&O) ALGORITHM

MPPT monitoring methods are often used in wind power generation to maximize power harvesting from renewable energy sources. MPPT is used to optimize the generator voltage through a rectifier at the boost converter location [21]. The working principle of MPPT P&O is shown in Figure 3.

TABLE I
WIND TURBINE PARAMETERS

Parameters	Quantities and Units
Nominal mechanical output power	3,000 W
Base power of the electrical generator	3,000/0.9 VA
Base wind speed	12 m/d
Maximum power at base wind speed of nominal mechanical pow	1 p.u
Base rotational speed of base generator	1.3 p.u
Pitch angle beta to display wind turbine power characteristics	0°

TABLE II
PARAMETER PMSG

Parameters	Quantities and Units
Number of phases	3
Back electromotive force (EMF) waveform	Sinusoidal
Rotor type	Round
Mechanical input	Torsi (Tm)
Stator phase resistance	0.4578 Ω
Inductance armature	0.00334 H
Voltage DC	300 V
Rpm	2,300 Rpm
Torque	10 Nm-14.2 Nm

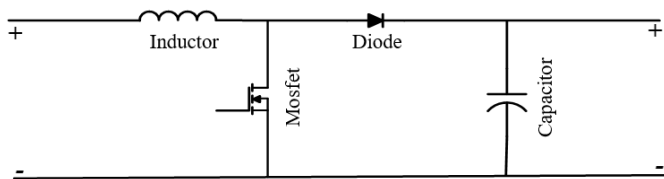


Figure 2. Boost converter circuit.

The algorithm used has an iterative nature, namely the calculation and adjustment of values are carried out repeatedly. This iteration process allows the system to adaptively respond to changing operating conditions. This algorithm started by reading the voltage (V) and current (I) values as inputs. Next, the power (P) was calculated, followed by the calculation of the voltage change (ΔV) and the power change (ΔP) for each iteration. Based on the ΔV and ΔP values, the algorithm would adjust the optimal duty cycle (D) value. This process would repeat continuously until the maximum power point was met.

F. DC-DC BIDIRECTIONAL CONVERTER

Bidirectional dc-dc converters can transfer power from the source side to the load side or vice versa [22]. They are different from dc-dc converters such as buck and boost converters. This is because bidirectional converters do not have diodes that prevent the current flow from reversing direction.

1) BUCK MODE

Bidirectional dc-dc converters operate like regular buck converters in this mode. Output voltages have lower values than input voltages. The relationship between the output voltage (V_o) and the input voltage (V_s) in buck mode is expressed by (8).

$$V_o = V_s \times D. \quad (8)$$

The capacitor outputs (C) and minimum inductor (L_{min}) in the buck converters are expressed by (9) and (10) [15].

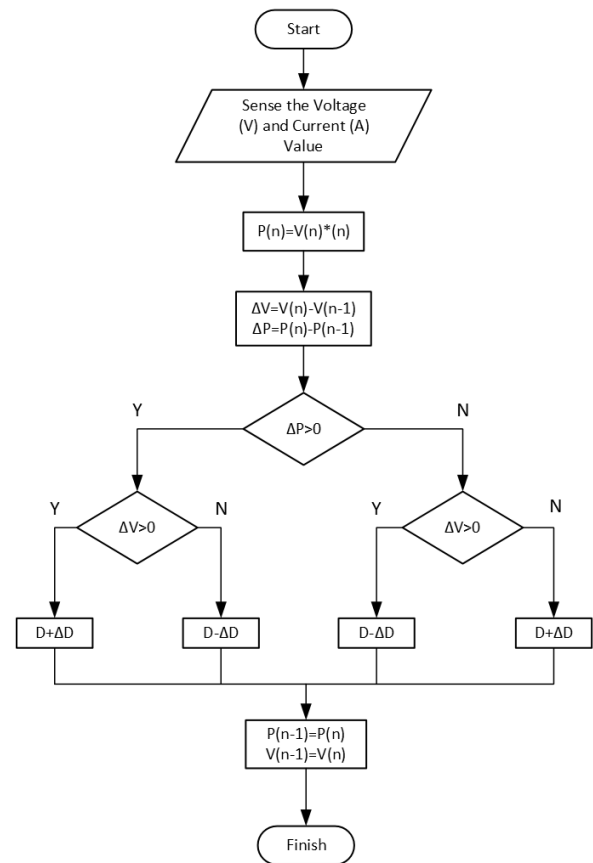


Figure 3. Working principle of P&O method.

$$L_{min} = \frac{(1-D) \times R}{2 \times f_s} \quad (9)$$

$$C_{min} = \frac{\Delta Q}{\Delta V_o} = \frac{\Delta iL \times T}{8 \Delta V_o} = \frac{\Delta iL}{8 \times f_s \times \Delta V_o}. \quad (10)$$

2) BOOST MODE

In this mode, the bidirectional dc-dc converters operate like regular boost converters. The output voltage value is higher than that of input voltage. The relationship between the output voltage (V_o) and the input voltage (V_s) is indicated by (5) and the value of the low-voltage side capacitor is indicated by (7).

The bidirectional dc-dc converter mode depends on the dc bus voltage. The set point of the dc bus is 400 V. When the amount of energy generated by the wind turbine exceeds the load demand, the dc bus will have a voltage of 400 V and the bidirectional dc-dc converter operates on buck mode to charge the battery. However, the bidirectional dc-dc converter operates on boost mode, indicating that the dc bus will undergo a voltage drop due to the wind turbine's power being lower than the load demand. Consequently, the dc bus will experience a voltage drop. The bidirectional dc-dc converter used had parameters of a switching frequency (f_s) of 5,000 Hz, inductor (L) of 0.004 H, a low-voltage side capacitor of 0.000625 F, and a high-voltage side capacitor of 0.000625 F.

G. PI CONTROL

The bidirectional dc-dc converter, operating in continuous conduction mode (CCM), controls the dc by regulating the duty cycle. On both the boost and the buck sides, the PI control maintains a constant voltage. As shown in Figure 4, the PI control loop forms this control. The feedback signal to the PI control is the output voltage (V_{KB}). The external voltage loop

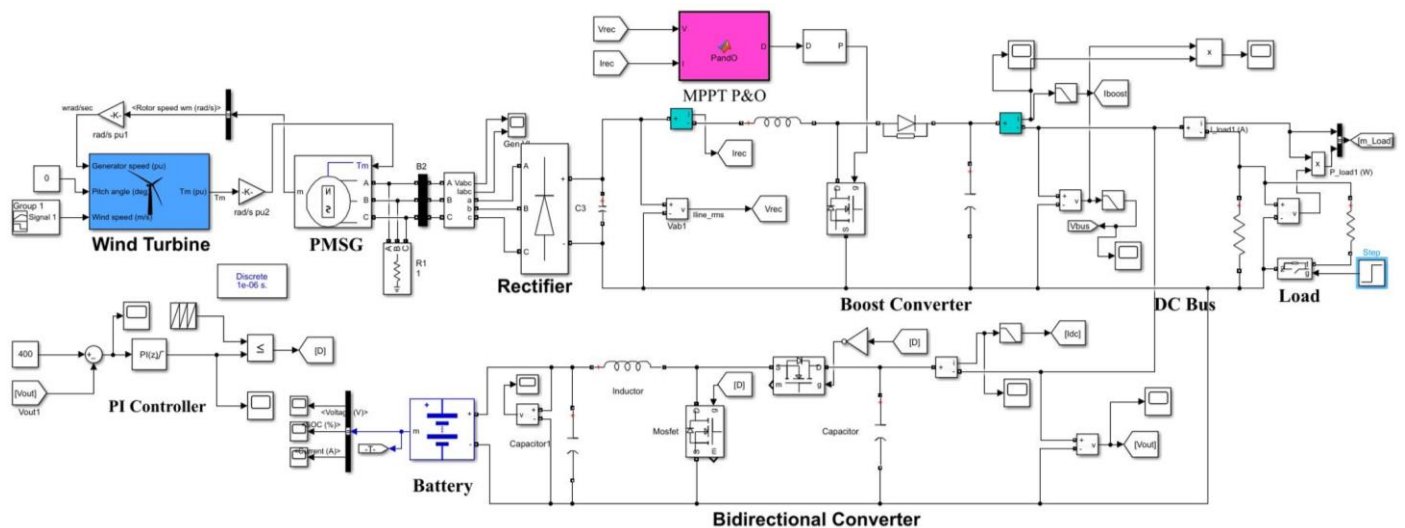


Figure 4. Simulation model of the design of a wind turbine-battery-based dc microgrid voltage regulation system capacity on Simulink MATLAB.

provides a reference for the PI control loop. In the external voltage loop, V_{KB} is obtained and compared to the reference voltage (V_{ref}). The PI control handles the difference between the two. To obtain the duty cycle, the PI control processes the difference to generate a stable voltage for the dc bus supply on the high-voltage side.

H. BATTERY

A battery is a tool that can convert chemical energy in the battery into electrical energy. Basically, a battery is a machine that converts chemical energy in its active material into electrical energy through an electrochemical redox reaction or oxidation-reduction. A battery consists of an electrolyte, which serves as a conductor as well as positive and negative terminals. The output current from the battery is dc current. The energy storage system unit in the United States microgrid system is designed to provide a stable voltage to the load under changing load conditions. Since the power generated by the wind turbine does not always meet the required load, the battery that functions as energy storage can help meet the load demand. In this case, the battery state-of-charge (SoC) system is considered to be in the range of 50% with a battery capacity of 200 Ah.

I. LOAD

In designing a wind turbine-battery-based dc microgrid voltage regulation system, resistive loads were used to test the system's reliability. There are two variations of resistive loads, each with a load of 1,000 W. The first load variation was directly connected to the designed system. On the other hand, the second load variation was connected to the system at the third second, resulting in the total load of 2,000 W. Therefore, the reliability of the designed system could be analyzed.

J. IEC 61000-4-17

IEC 61000-4-17 is an international standard for electromagnetic compatibility (EMC) testing, specifically addressing disturbances caused by transient dc voltages. This standard outlines the method for testing the resistance of electrical or electronic equipment to ripple in the input dc power. It applies to low-voltage dc power in equipment supplied by an external rectifier system, or a battery being charged. The IEC 61000-4-17 standard permits a ripple voltage of up to 1% of the nominal voltage in dc electronic equipment.

These standard covers voltage waveforms, ranges, settings, and test procedures.

III. RESULTS AND DISCUSSION

This section outlines the testing results of the design of the wind turbine-battery-based dc microgrid voltage regulation system. The proposed system was simulated for 5 s using Simulink MATLAB. The simulation circuit model is shown in Figure 4.

The wind turbine capacity used was 3 kW. In this study, there were three variations of wind speed, each representing a particular condition. The first variation is the wind speed of 12 m/s. In this condition, the wind power plant entirely supplied the load, and excess power from the plant was used to charge the battery. The second variation is the wind speed of 8 m/s. In this wind speed condition, the power generated by the plant was not optimal, so the existing battery played an active role in assisting the wind power plant to supply the load. In the third variation with a wind speed being 4 m/s, the wind power plant was unable to generate any power at all. Hence, the battery entirely supplied the existing load. This study also carried out tests with additional loads when each condition took place. It aimed to determine the voltage regulation performance of the designed dc bus.

A. LOAD AND BATTERY SUPPLIED BY WIND TURBINES

Figure 5 shows a wind turbine power, load, and bidirectional dc-dc converter graph. Based on the simulation results that had been carried out, the output power of the wind turbine with a wind speed of 12 m/s was 3,600 W. Figure 5 shows that the output power of the wind turbine has a non-constant value, and oscillations occur continuously. It is a power tracking process carried out by the boost converter with the MPPT P&O algorithm so that the power generated will continuously oscillate to obtain the maximum output power of the wind turbine. The wind turbine could supply the load and charge the battery with a wind speed of 12 m/s. It can be seen in Figure 5 that the power in the bidirectional dc-dc converter operates in buck mode for battery charging, as evidenced by the battery power, which has a negative value indicating the process of charging the battery. Oscillation occurred in the battery charging process because the input coming from the wind turbine oscillated as well. At the third second in the

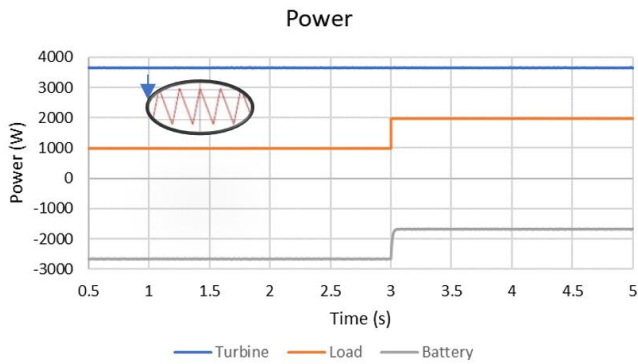


Figure 5. Wind turbine output, load, and battery power when the wind speed is 12 m/s.

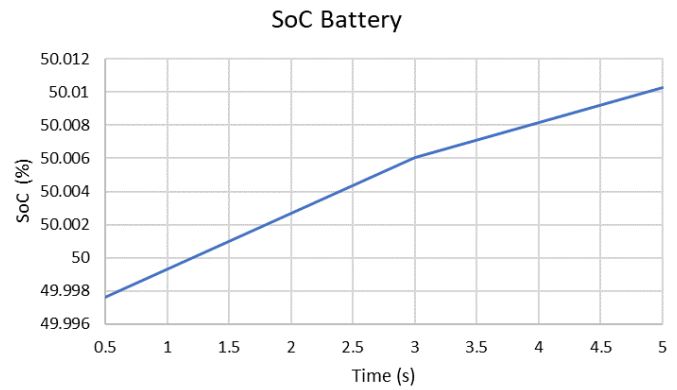


Figure 7. SoC battery when the wind speed is 12 m/s.

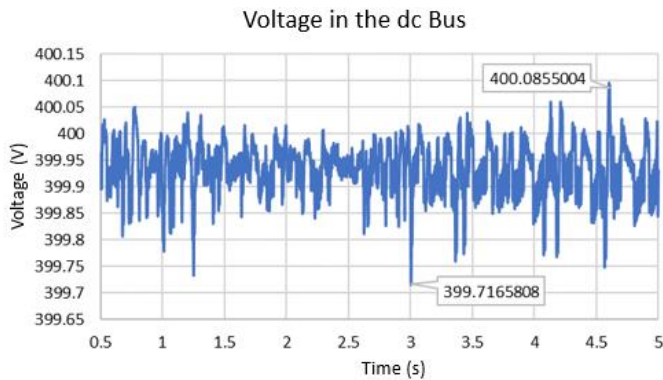


Figure 6. Dc bus voltage when the wind speed is 12 m/s.

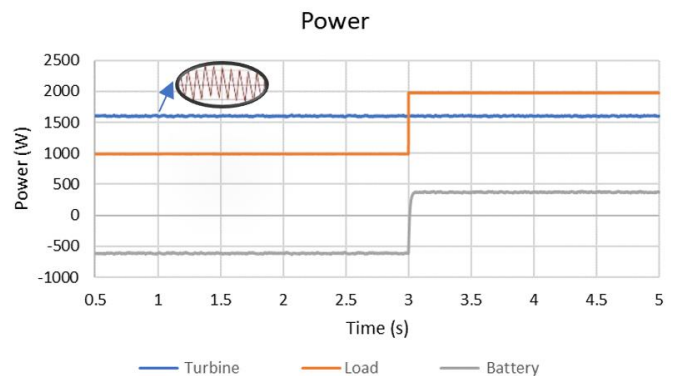


Figure 8. Wind turbine output, load, and battery power when the wind speed is 8 m/s.

simulation, the load on the system increased from 1,000 W to 2,000 W. When the load increased, the output power of the wind turbine remained unchanged. The difference can be seen in the existing battery power. The initial power input to the battery was -2,500 W, then it became -1,500 W.

Figure 6 illustrates the voltage graph on the dc bus of the microgrid system with a wind speed of 12 m/s. When the wind turbine supplied the load and charged the battery, the voltage on the dc bus of the microgrid system could maintain the voltage at a level of 400 V. In the third second, there was an additional load on the system, causing the voltage value to drop slightly and subsequently return to the level of 400 V. The measurement results of the dc bus's lowest and the highest voltages immediately after the addition of the load in the third second were 399.7 V and 400 V. Hence, the voltage fluctuation of the dc bus was 0.3 V. The dc bus could maintain the voltage at a level of 400 V despite the additional load in the third second. The dc bus could maintain a voltage level of 400 V, with a voltage ripple of 0.3 V (0.075% of the nominal voltage). According to the IEC 61000-4-17 standard, this voltage ripple remains within the acceptable tolerance limit for dc electronic equipment, which is below 1%.

Figure 7 presents the SoC battery graph. With a wind speed of 12 m/s, the wind turbine could supply the load while charging the battery. The SoC battery value increased over time. In the third second, there was an additional load on the system, resulting in the power used to charge the battery getting smaller. Figure 7 shows that after the third second, the SoC battery curve is getting flatter compared to the previous second.

B. LOAD SUPPLIED BY WIND TURBINES AND BATTERIES

Figure 8 shows a wind turbine power, load, and bidirectional dc-dc converter graph. Based on the simulation

results that had been carried out, the output power of the wind turbine with a wind speed of 8 m/s was around 1,600 W. Figure 8 shows that the output power of the wind turbine has a non-constant value, and oscillations occur continuously. This occurs because the power tracking process is carried out by the boost converter with the MPPT P&O algorithm so that the power generated will continuously oscillate to obtain the maximum output power of the wind turbine. With a wind speed of 8 m/s, the wind turbine was incapable of supplying the load, so in this system, the battery also had a role in supplying the load. This can be seen in Figure 8. The bidirectional dc-dc converter provided power to the load in boost mode, indicating a positive battery power value. At the third second in the simulation, the load on the system increased from 1,000 W to 2,000 W. When the load increased, the output power of the wind turbine remained unchanged as the maximum power achievable at a wind speed of 8 m/s was 1,600 W. The difference can be seen from the power on the bidirectional dc-dc converter, namely the output power from the battery, which was initially -600 W, changed to 400 W.

Figure 9 shows the voltage graph on the dc bus of the microgrid system with a wind speed of 8 m/s. The microgrid system could maintain the voltage on the dc bus at 400 V when the wind turbine and battery supplied the load. In the third second, there was an additional load on the system, causing the voltage value to drop slightly and subsequently return to the level of 400 V. The measurement results of the dc bus's lowest and the highest voltages immediately after the addition of the load in the third second were 399.8 V and 400.1. Hence, the fluctuation of the dc bus voltage was 0.3 V. The wind turbine and battery could maintain the dc bus voltage at 400 V, and the supply to the load was not interrupted. The dc bus could

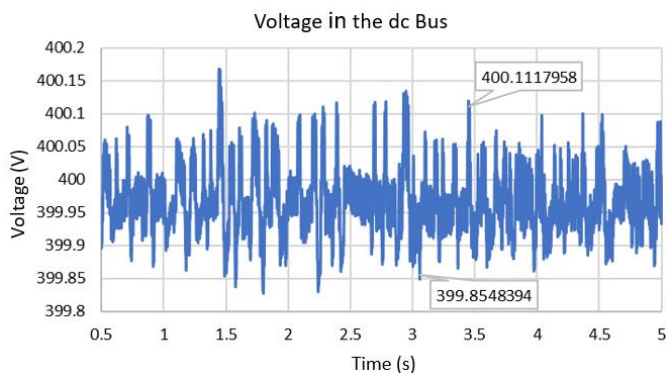


Figure 9. Bus voltage when the wind speed is 8 m/s.

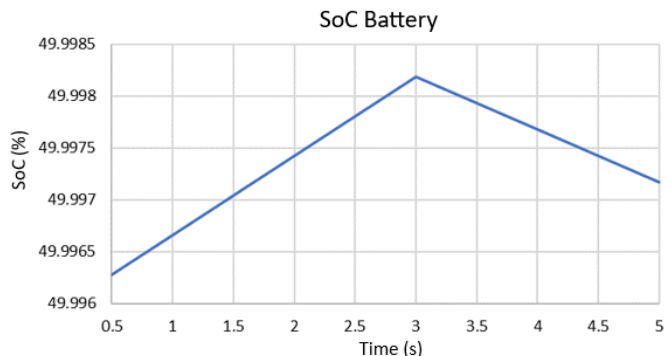


Figure 10. SoC battery when the wind speed is 8 m/s.

maintain a voltage level of 400 V, with a voltage ripple of 0.3 V (0.075% of the nominal voltage). According to the IEC 61000-4-17 standard, the voltage ripple is still within the acceptable tolerance limit for the dc electronic equipment, which is below 1%.

Figure 10 illustrates the graph of the SoC battery. With a wind speed of 8 m/s, the battery needed to contribute to supplying the load because the maximum output power of the wind turbine was not enough to fully supply the load. The SoC battery value decreased over time. In the third second, the system experienced an increase in load, prompting an increase in the battery output power to supply the load. Figure 10 shows that after the third second, the SoC battery curve is steeper compared to the previous second.

C. LOAD SUPPLIED BY BATTERIES

Figure 11 shows a graph of wind turbine power, load, and bidirectional dc-dc converter. Based on the simulation results that had been carried out, the wind turbine could not produce output power when the wind speed was 4 m/s. At this wind speed, the load on the system was fully supplied by the battery. Figure 11 shows that the bidirectional dc-dc converter works in boost mode to supply the load, as evidenced by the positive battery power. In the third second of the simulation, the load on the system increased from 1,000 W to 2,000 W. When the load increased, the output power from the battery also changed, the same as the power on the load. It indicates that the battery fully supplies the load.

Figure 12 illustrates the voltage graph on the dc bus of the microgrid system with a wind speed of 4 m/s. When the battery entirely supplied the load, the voltage on the dc bus of the microgrid system can be maintained at a level of 400 V. In the third second, there was an additional load on the system, causing the voltage value to drop slightly and subsequently return to the level of 400 V. The measurement results indicated

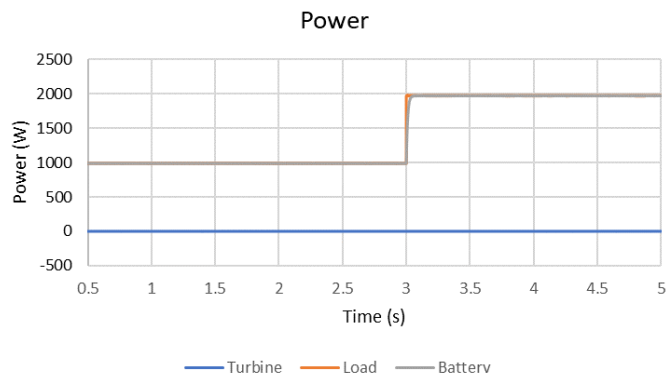


Figure 11. Wind turbine output, load, and battery power when the wind speed is 4 m/s.

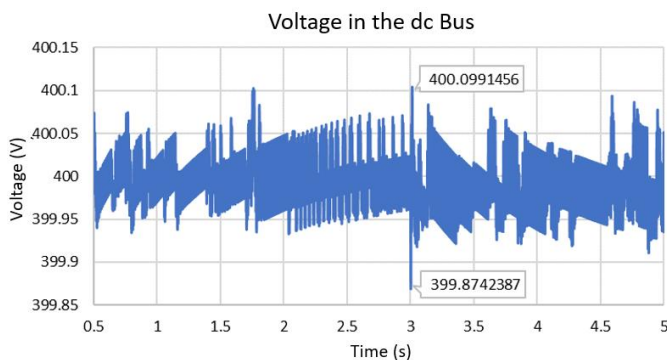


Figure 12. Dc bus voltage when the wind speed 4 m/s.

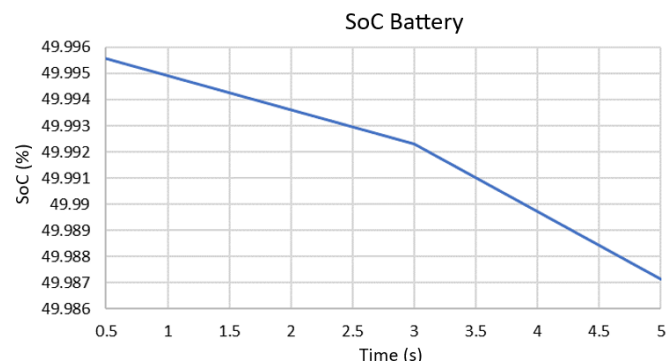


Figure 13. SoC battery when the wind speed is 4 m/s.

that the lowest and highest voltages of the dc bus immediately after the addition of the load in the third second were 399.8 V and 400 V. Hence, the fluctuation of the dc bus voltage was 0.2 V. The battery could maintain the dc bus voltage at a level of 400 V and the supply to the load was not interrupted. The dc bus could maintain a voltage level of 400 V, with a voltage ripple of 0.2 V (0.05% of the nominal voltage). According to the IEC 61000-4-17 standard, this voltage ripple remains within the acceptable tolerance limit for the dc electronic equipment, which is below 1%.

Figure 13 displays the graph of the SoC battery. With a wind speed of 4 m/s, the battery completely supplied the load because the wind turbine could not generate power. It can be seen that the SoC battery value decreases over time. The SoC curve with this wind speed is steeper compared to the SoC curve at a wind speed of 8 m/s. In the third second, there was an additional load on the system, causing an increase in the battery output power to supply the load. Figure 13 shows that after the 3rd second, the SoC curve on the battery is steeper compared to the previous second.

IV. CONCLUSION

The performance of the designed dc microgrid system can operate well. The output power of the wind turbine can meet the load demand and charge the battery. When the turbine cannot generate output power, the battery can meet the load demand. The test results showed that at a wind speed of 12 m/s, the wind turbine could generate electricity to meet the load demand and charge the battery. At a wind speed of 8 m/s, the battery could supply the lack of turbine output power to meet the load demand. At a wind speed of 4 m/s, the wind turbine failed to generate output power, and the battery entirely supplied the load. The proposed system successfully maintained the voltage on the dc bus at 400 V with a deviation of only 1%. Based on the IEC 61000-4-17 reference, these values remain below the load tolerance limit.

CONFLICTS OF INTEREST

The authors declare that there are no conflicts of interest in this research.

AUTHORS' CONTRIBUTIONS

Conceptualization, Sidiq Budi Perkasa; methodology, Sidiq Budi Perkasa; software, Sidiq Budi Perkasa; validation, Sidiq Budi Perkasa, Mochammad Facta, and Iwan Setiawan; formal analysis, Sidiq Budi Perkasa, Mochammad Facta, and Iwan Setiawan; investigation, Sidiq Budi Perkasa, Mochammad Facta, and Iwan Setiawan; resources, Sidiq Budi Perkasa; writing—original draft preparation, Sidiq Budi Perkasa; writing—reviewing and editing, Sidiq Budi Perkasa, Mochammad Facta, and Iwan Setiawan; visualization, Sidiq Budi Perkasa; supervision, Mochammad Facta and Iwan Setiawan.

ACKNOWLEDGMENT

The authors would like to express our deepest gratitude to all parties who have helped and supported us during the process of writing this paper.

REFERENCES

- [1] A. Hamza, H. Bin Tahir, K. Siraj, and M. Nasir, "Hybrid ac/dc microgrid for residential applications," in *2019 IEEE 3rd Int. Conf. DC Microgrids (ICDCM)*, 2019, pp. 1–5, doi: 10.1109/icdcm45535.2019.9232773.
- [2] S. Pannala, N. Patari, A.K. Srivastava, and N.P. Padhy, "Effective control and management scheme for isolated and grid connected dc microgrid," *IEEE Trans. Ind. Appl.*, vol. 56, no. 6, pp. 6767–6780, Nov/Dec. 2020, doi: 10.1109/TIA.2020.3015819.
- [3] J. Dhillon and A.K. Kouam, "Design and modelling of a dc microgrid for wind and solar system," in *2022 1st Int. Conf. Sustain. Technol. Power Energy Syst.*, 2022, pp. 1–6, doi: 10.1109/stpes54845.2022.10006534.
- [4] N. Qachchachi, H. Mahmoudi, and A.E. Hassnaoui, "Control strategy of hybrid ac/dc microgrid in standalone mode," *Int. J. Renew. Energy Dev.*, vol. 9, no. 2, pp. 295–301, Jul. 2020, doi: 10.14710/ijred.9.2.295-301.
- [5] W. Bai, "DC microgrid optimized energy management and real-time control of power systems for grid-connected and off-grid operating modes," Disertasi Ph.D., Université de Technologie de Compiègne, Compiègne, Perancis, 2021.
- [6] S. Abdullahi, T. Jin, and P.M. Lingom, "Robust control strategy for inductive parametric uncertainties of dc/dc converters in islanded dc microgrid," *J. Mod. Power Syst. Clean Energy*, vol. 11, no. 1, pp. 335–344, Jan. 2023, doi: 10.35833/MPCE.2021.000241.
- [7] J. Aourir, F. Locment, and M. Sechilariu, "Power and energy management of a dc microgrid for a renewable curtailment case due to the integration of a small-scale wind turbine," *Energies*, vol. 15, no. 9, pp. 1–24, May 2022, doi: 10.3390/en15093421.
- [8] M.F.N. Akbar, Z. Zulfatman, and I. Pakaya. (22 Dec. 2020). Maximum power point tracking pada pembangkit tenaga angin menggunakan backtracking search algorithm. Dipresentasikan pada Semin. Nas. Teknol. Rekayasa (SENTRA), [Online], <https://www.youtube.com/watch?v=jPPqToVHeoU>
- [9] K.R. Bharath, M.M. Krishnan, and P. Kanakasabapathy, "A review on dc microgrid control techniques, applications and trends," *Int. J. Renew. Energy Res.*, vol. 9, no. 3, pp. 1328–1338, Sep. 2019, doi: 10.20508/ijrer.v9i3.9671.g7710.
- [10] H. Chen, "Lithium-ion battery-supercapacitor energy management for dc microgrids," *Int. J. Low-Carbon Technol.*, vol. 17, pp. 1452–1458, Nov. 2022, doi: 10.1093/ijlct/ctac128.
- [11] R. Rajasekaran and P.U. Rani, "Bidirectional dc-dc converter for microgrid in energy management system," *Int. J. Electron.*, vol. 108, no. 2, pp. 322–343, Feb. 2021, doi: 10.1080/00207217.2020.1793418.
- [12] V.F. Pires, A. Pires, and A. Cordeiro, "DC microgrids: Benefits, architectures, perspectives and challenges," *Energies*, vol. 16, no. 3, pp. 1–20, Feb. 2023, doi: 10.3390/en16031217.
- [13] A. Kusmanto, A. Priyadi, V.L.B. Putri, and M.H. Purnomo, "Kinerja micro grid menggunakan photovoltaic-baterai dengan sistem off-grid," *J. Nas. Tek. Elekt. Teknol. Inf.*, vol. 9, no. 2, pp. 211–217, May 2020, doi: 10.22146/jnteti.v9i2.155.
- [14] A. Kusmanto and A. Priyadi, "Strategi peningkatan kinerja dc microgrid dengan konfigurasi dc/ac coupling," *J. Nas. Tek. Elekt. Teknol. Inf.*, vol. 12, no. 3, pp. 175–180, Aug. 2023, doi: 10.22146/jnteti.v12i3.7151.
- [15] A.M. Yasin, "Energy management of a stand-alone dc microgrid based on PV/wind/battery/diesel gen. combined with super-capacitor," *Int. J. Renew. Energy Res.*, vol. 9, no. 4, pp. 1811–1826, Dec. 2019, doi: 10.20508/ijrer.v9i4.10094.g7784.
- [16] G.S. Mahesh, A. Puskar, P. M. Krishna, and S. Rajashekhar, "Energy management with bi-directional converters in dc microgrids," in *Int. Conf. Thermo-fluids Energy Syst. (ICTES2019)*, 2020, pp. 1–8, doi: 10.1088/1742-6596/1473/1/012016.
- [17] V. Patel and V. Patel, "A comprehensive review: Ac & dc microgrid protection," in *21st Natl. Power Syst. Conf. (NPSC)*, 2020, pp. 1–6, doi: 10.1109/NPSC49263.2020.9331932.
- [18] H. Piggott, *Windpower Workshop*. Machynlleth, Inggris: Centre for Alternative Technol, 1997.
- [19] D.W. Hart, *Power Electronics*. New York, NY, USA: McGraw-Hill, 2010.
- [20] M.S. Simoiu *et al.*, "BOOST converter modelling as a subsystem of a photovoltaic panel control system," in *2020 IEEE Int. Conf. Autom. Qual. Test. Robot. (AQTR)*, 2020, pp. 1–6, doi: 10.1109/AQTR49680.2020.9129963.
- [21] R. Syahputra and I. Soesanti, "Performance improvement for small-scale wind turbine system based on maximum power point tracking control," *Energies*, vol. 12, no. 20, pp. 1–18, Oct. 2019, doi: 10.3390/en12203938.
- [22] A.S. Pratiwi, S.D. Nugraha, and E. Sunarno, "Desain dan simulasi bidirectional dc-dc converter untuk penyimpanan energi pada sistem fotovoltaik," *J. Nas. Tek. Elekt. Teknol. Inf.*, vol. 9, no. 3, pp. 305–310, Aug. 2020, doi: 10.22146/v9i3.377.